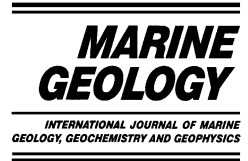




ELSEVIER

Marine Geology 189 (2002) 5–23



www.elsevier.com/locate/margeo

Astronomical age models for Pleistocene drift sediments from the western North Atlantic (ODP Sites 1055–1063)

J. Grützner^{a,*}, L. Giosan^b, S.O. Franz^c, R. Tiedemann^a, E. Cortijo^d,
W.P. Chaisson^e, R.D. Flood^b, S. Hagen^f, L.D. Keigwin^g, S. Poli^h, D. Rioⁱ,
T. Williams^j

^a GEOMAR-Forschungszentrum für marine Geowissenschaften, Wischhofstrasse 1–3, 24148 Kiel, Germany

^b Marine Sciences Research Center, State University of New York, Stony Brook, Stony Brook, NY 11794-5000, USA

^c Geologisches Institut, Universität Bonn, Nussallee 8, 53115 Bonn, Germany

^d Centre des Faibles Radioactivités (CFR) (UPR 2101), CNRS, Avenue de la Terrasse, Gif-sur-Yvette Cedex 91198, France

^e Department of Earth and Environmental Sciences, University of Rochester, Rochester, NY 14627, USA

^f Institute of Biology and Geology, Department of Geology, Universitetet i Tromsø, 9037 Tromsø, Norway

^g Woods Hole Oceanographic Institution, McLean Laboratory, MS 8, 360 Woods Hole Road, Woods Hole, MA 02543, USA

^h Department of Geography and Geology, Eastern Michigan University, Ypsilanti, MI, USA

ⁱ Dipartimento di Geologia Paleontologia e Geofisica, Università degli Studi di Padova, Via Giotto 1, 35137 Padova, Italy

^j Borehole Research Group, Lamont–Doherty Earth Observatory, Palisades, NY 10964, USA

Received 15 May 2000; accepted 25 January 2002

Abstract

Ten ODP sites drilled in a depth transect (2164–4775 m water depth) during Leg 172 recovered high-deposition rate (> 20 cm/kyr) sedimentary sections from sediment drifts in the western North Atlantic. For each site an age model covering the past 0.8–0.9 Ma has been developed. The time scales have a resolution of 10–20 kyr and are derived by tuning variations of estimated carbonate content to the orbital parameters precession and obliquity. Based on the similarity in the signature of proxy records and the spectral character of the time series, the sites are divided into two groups: precession cycles are better developed in carbonate records from a group of shallow sites (2164–2975 m water depth, Sites 1055–1058) while the deeper sites (2995–4775 m water depth, Sites 1060–1063) are characterized by higher spectral density in the obliquity band. The resulting time scales show excellent coherence with other dated carbonate and isotope records from low latitudes. Besides the typical Milankovitch cyclicity significant variance of the resulting carbonate time series is concentrated at millennial-scale changes with periods of about 12, 6, 4, 2.5, and 1.5 kyr. Comparisons of carbonate records from the Blake Bahama Outer Ridge and the Bermuda Rise reveal a remarkable similarity in the time and frequency domain indicating a basin-wide uniform sedimentation pattern during the last 0.9 Ma. © 2002 Elsevier Science B.V. All rights reserved.

Keywords: Pleistocene time scale; astronomical chronology; western North Atlantic; drift sediments; Ocean Drilling Program

* Corresponding author. Present address: Fachbereich Geowissenschaften Universität Bremen, Postfach 33 04 40, 28334 Bremen, Germany. Tel.: +49-421-2182482.

E-mail address: jgruetzn@allgeo.uni-bremen.de (J. Grützner).

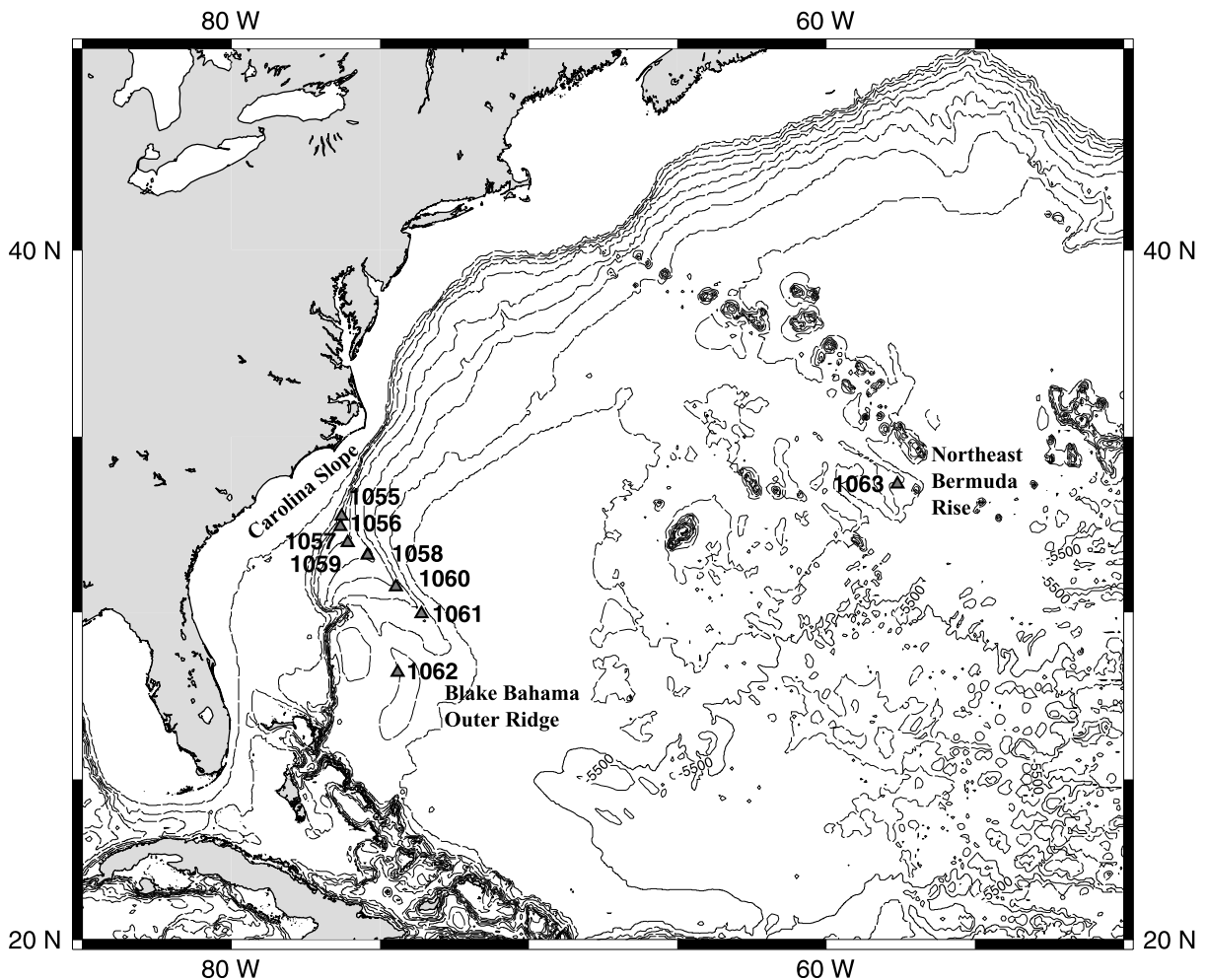


Fig. 1. Location of nine ODP sites drilled during Leg 172 on the Carolina Slope (Site 1055), the Blake Bahama Outer Ridge (Sites 1056–1062) and the Bermuda Rise (Site 1063). Astronomically tuned age models are presented for these sites.

1. Introduction

The astronomical theory of climate first formulated by Milutin Milankovitch (1920, 1941) provided not only deep insights into the mechanisms of global climatic change but also opened the way for the creation of accurate high-resolution geochronologies. After Hays et al. (1976) had shown that variations in the earth's orbital geometry are responsible for climatic changes which can be documented in sedimentary records, time scales have been developed by correlating paleoclimatic indicators to astronomical forcing functions (e.g. Johnson, 1982; Imbrie et al., 1984; Martinson et

al., 1987). Meanwhile, these chronologies have been extended and modified in some cases (Shackleton et al., 1990; Tiedemann et al., 1994; Bassinot et al., 1994; Berger et al., 1995). The astronomical dating technique is called 'orbital tuning' and has a theoretical accuracy of a few thousand yr (Martinson et al., 1987). Most of the new age models were created by the correlation of isotopic records (^{18}O – ^{16}O in tests of fossil foraminifera) with orbital target curves (e.g. Imbrie et al., 1984; Shackleton et al., 1990). However, if isotopic data were lacking, other climate proxies like bulk density, magnetic susceptibility, or carbonate content have been successfully used

(e.g. Shackleton et al., 1995; Bickert et al., 1997; Tiedemann and Franz, 1997; Ortiz et al., 1999). As tuning targets several different forcing functions such as insolation, ice volume models, precession or obliquity have been used. Martinson et al. (1987) tested four different tuning approaches with a stacked isotope data set and demonstrated that the chronology produced is insensitive to the specific tuning technique used.

In this study we present orbitally (precession and obliquity) tuned age models for the Pleistocene (0–0.9 Ma) of ten ODP sites in the western North Atlantic based on carbonate content records. The sites drilled in a depth transect (2164–4775 m water depth) during Leg 172 recovered high-deposition rate (>20 cm/kyr) sedimentary sections from sediment drifts and provide an archive to study millennial-scale climate changes as

well as variations in the depth distribution of Atlantic water masses (Keigwin et al., 1998). The age models developed here are an important prerequisite for detailed comparisons of proxy records from the different locations. In this paper we use them to compare suborbital (<19 kyr) climatic variability at the Blake Bahama Outer Ridge and at the Bermuda Rise.

2. Materials, data and initial dating

Fig. 1 shows the locations of nine ODP sites drilled during Leg 172 on the Carolina Slope (Site 1055), the Blake Bahama Outer Ridge (Sites 1056 to 1062) and the Bermuda Rise (Site 1063). Multiple holes were drilled at each site so that the continuity of recovery was confirmed by the de-

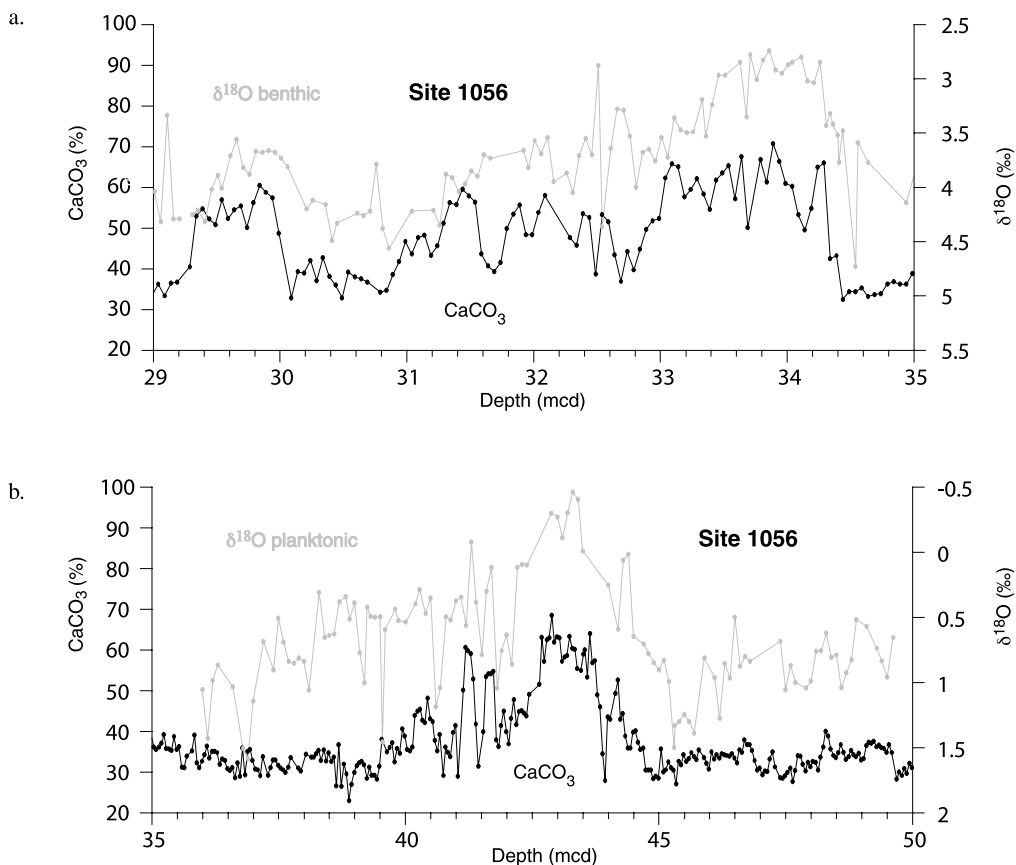


Fig. 2. Comparison of the carbonate record from Site 1056 to first results from oxygen isotope measurements on benthic (*N. dutertrei*) and planktonic (*C. wuellerstorfi*) foraminifera.

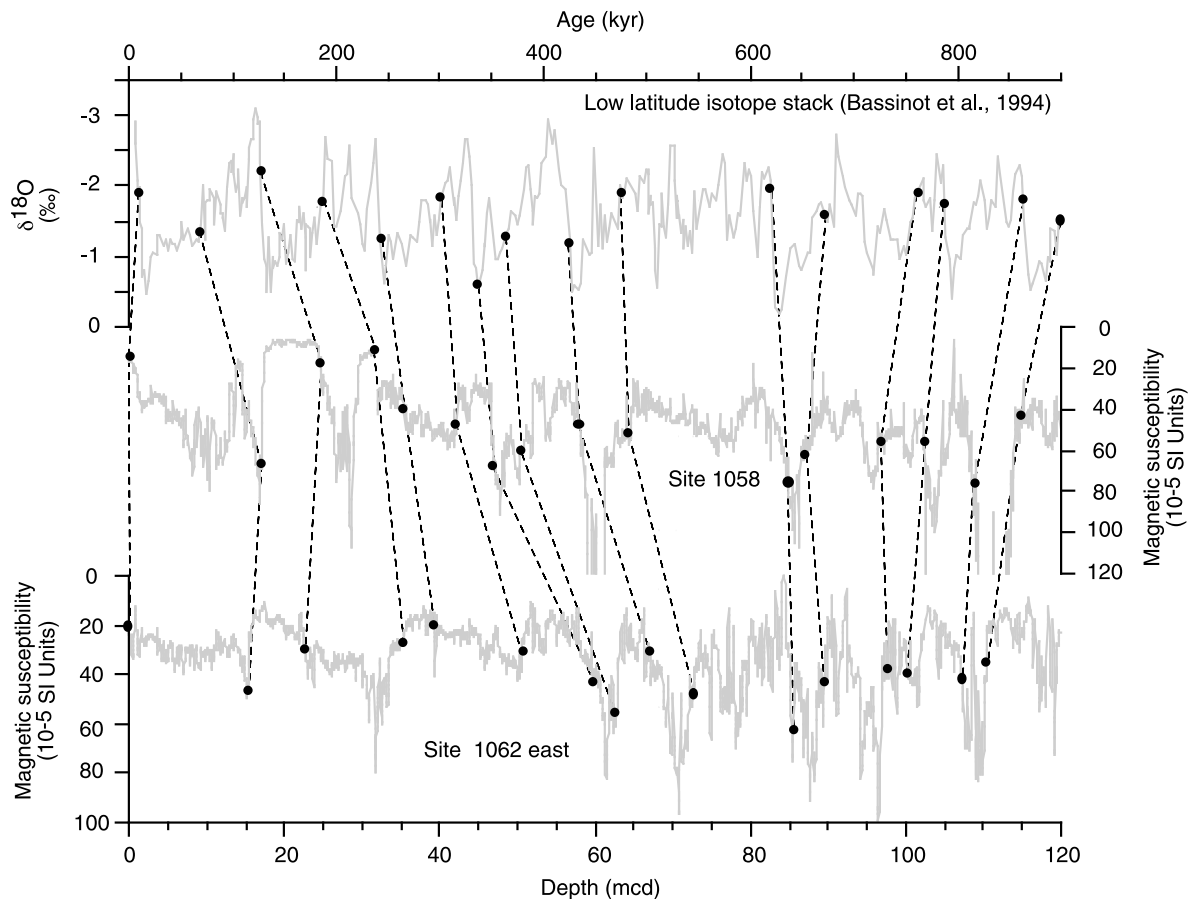


Fig. 3. Sites 1058 and 1062east were used as 'reference' sites for dating. The initial age models for these sites are based on the correlation of magnetic susceptibility records to an isotope stack for low latitudes (Bassinot et al., 1994).

velopment of composite depth sections (depth in meters composite depth, mcd) and splices (Shipboard Scientific Party, 1998a). At Site 1062, eight holes were drilled on either flank and into the crest of a mud wave at the base of the Bahama Outer Ridge. For this site we present two age models, one for the eastern (1062east) and one for the western part (1062west) of the mud wave.

All sites show a remarkably similar sediment composition, characterized by continuous sedimentation with cyclic alterations between nannofossil-rich and clay-rich sediments (Keigwin et al., 1998). Measured variations of lithological and physical parameters are similar to standard isotope curves and are obviously related to orbitally tuned climatic forcing. This is confirmed by first oxygen isotope results (Franz and Tiedemann,

2002; Chaisson et al., 2002) from Site 1056 which covers Marine Isotope Stages (MIS) 8–12 and was measured on planktonic (*N. dutertrei*) and benthic (*C. wuellerstorfi*) foraminifera. The $\delta^{18}\text{O}$ curves which primarily indicate variations in global ice volume, are in good correlation with the carbonate content record at Site 1056 (Fig. 2) indicating that variations in CaCO_3 content reflect glacial/interglacial variability. The sedimentation is characterized by the typical Atlantic-type pattern with higher CaCO_3 content during interglacial periods.

On the other hand, there are also important differences among the sites that are related to variable current strength, depth-dependent carbonate dissolution, distance from shore, and others (Shipboard Scientific Party, 1998b). Although lower carbonate accumulation due to higher dis-

solution is observed at the deeper sites, sedimentation rates show a drastic increase with water depth (> 20 cm/kyr) caused by higher detrital input. This suggests a higher sediment transport to the deeper sites caused by energetic deep ocean circulation. By examining the similarity in the signature of proxy records like susceptibility, bulk density (estimated from gamma ray attenuation) and color reflectance, the Leg 172 sites can be divided into two groups: the shallow Sites 1055–1059 and the deeper Sites 1060–1063.

As a first step in the orbital tuning procedure an initial age model for each site has been derived already during the cruise based on magnetic susceptibility measurements (Fig. 3). These initial age models rely on the similarity of the magnetic susceptibility records to a standard isotope curve for low latitudes (Bassinot et al., 1994). This isotope record represents a stack of data from ODP Site 677 in the equatorial Pacific (Shackleton et al., 1990) and from giant piston core MD9000963 in the tropical Indian Ocean. As tiepoints for the initial age models, 16 dated oxygen isotope events (stage boundaries) were used. The sedimentation rates are assumed constant between these age control points.

Although magnetic susceptibility is a first order

indicator of carbonate content, it is not an ideal tuning parameter for the Leg 172 sites because the susceptibility records are affected by reduction diagenesis of initial magnetic minerals (Schwartz et al., 1997). This is especially evident for the shallower sites (1055–1059) where magnetic susceptibility in the upper part of the sediment column (< 10 mbsf) is likely controlled by magnetite and is up to five times higher compared to the rest of the section. In deeper sections ferromagnetic minerals have been dissolved and the susceptibility signal is entirely swamped by paramagnetic clays (Shipboard Scientific Party, 1998c). However, glacial/interglacial variability is preserved because both magnetite and clay content reflect higher terrigenous input during colder climatic intervals. The shipboard initial age models were verified postcruise by using CaCO₃ records instead of magnetic susceptibility which resulted in very similar initial age models and identical final time scales.

Postcruise analyses have shown that a very accurate estimation of calcium carbonate content is possible by using diffuse spectral reflectance. Calibration of the reflectance records was obtained from stepwise multiple linear regression of the reflectance spectra with 4141 shipboard and post-

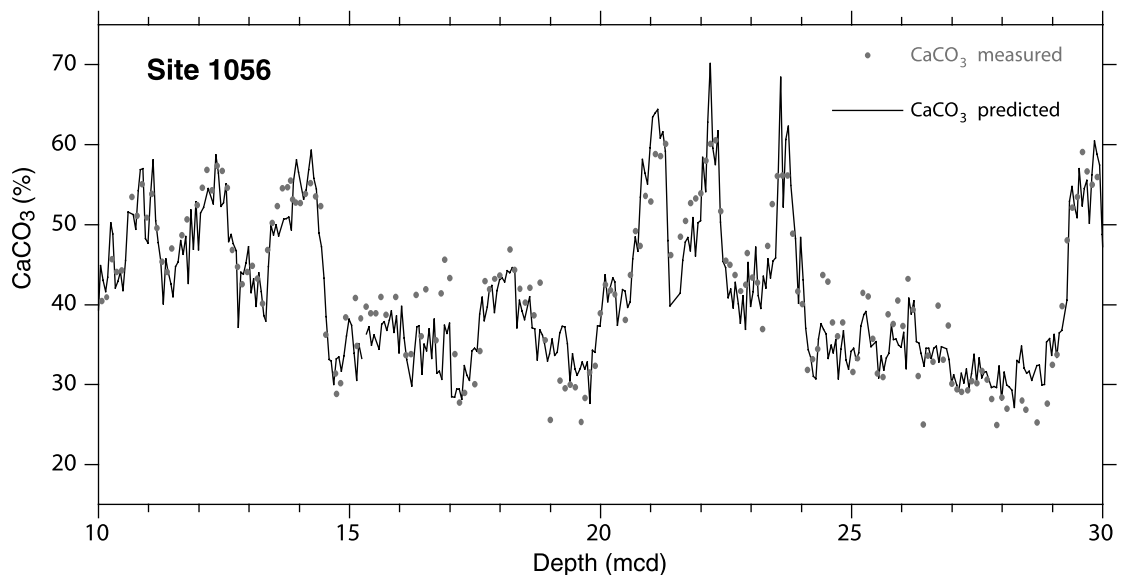


Fig. 4. Example from Site 1056 comparing the carbonate predictions derived from color reflectance data with CaCO₃ measurements (LECO-analyzer) on discrete samples.

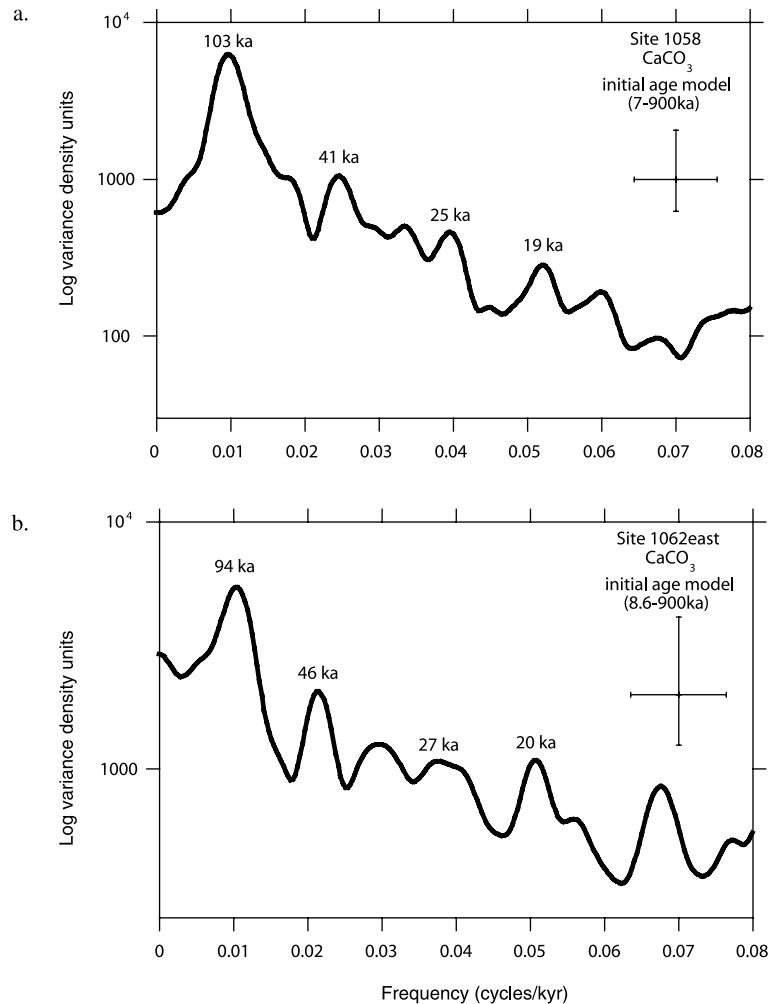


Fig. 5. Spectral analyses of carbonate time series based on shipboard age models reveal significant power spectral density close to Milankovitch periods of 100, 41 and 19–23 kyr.

cruise carbonate measurements (Giosan et al., 2001) resulting in carbonate estimations with root-mean-square-errors between 4 and 7%. An example for the carbonate prediction from Site 1056 is shown in Fig. 4. Therefore, our fine-tuning approach is based on high-resolution records (2–5-cm sample interval) of estimated calcium carbonate.

3. Astronomical calibration

Spectral analyses of the initial carbonate time

series (based on the initial age models) reveal significant power spectral density close to Milankovitch periods of 100, 41, and 19–23 kyr (Fig. 5) confirming that sedimentation changes in the western North Atlantic are linked to variations in earth orbital parameters. This is an important precondition for using the orbital time series of precession and obliquity as target curves to improve the initial age scales. The slight deviation of the variance density peaks from the Milankovitch periods can be explained by the low resolution of the initial age models and it also points to the need for a finer tuning. Thus to achieve higher-

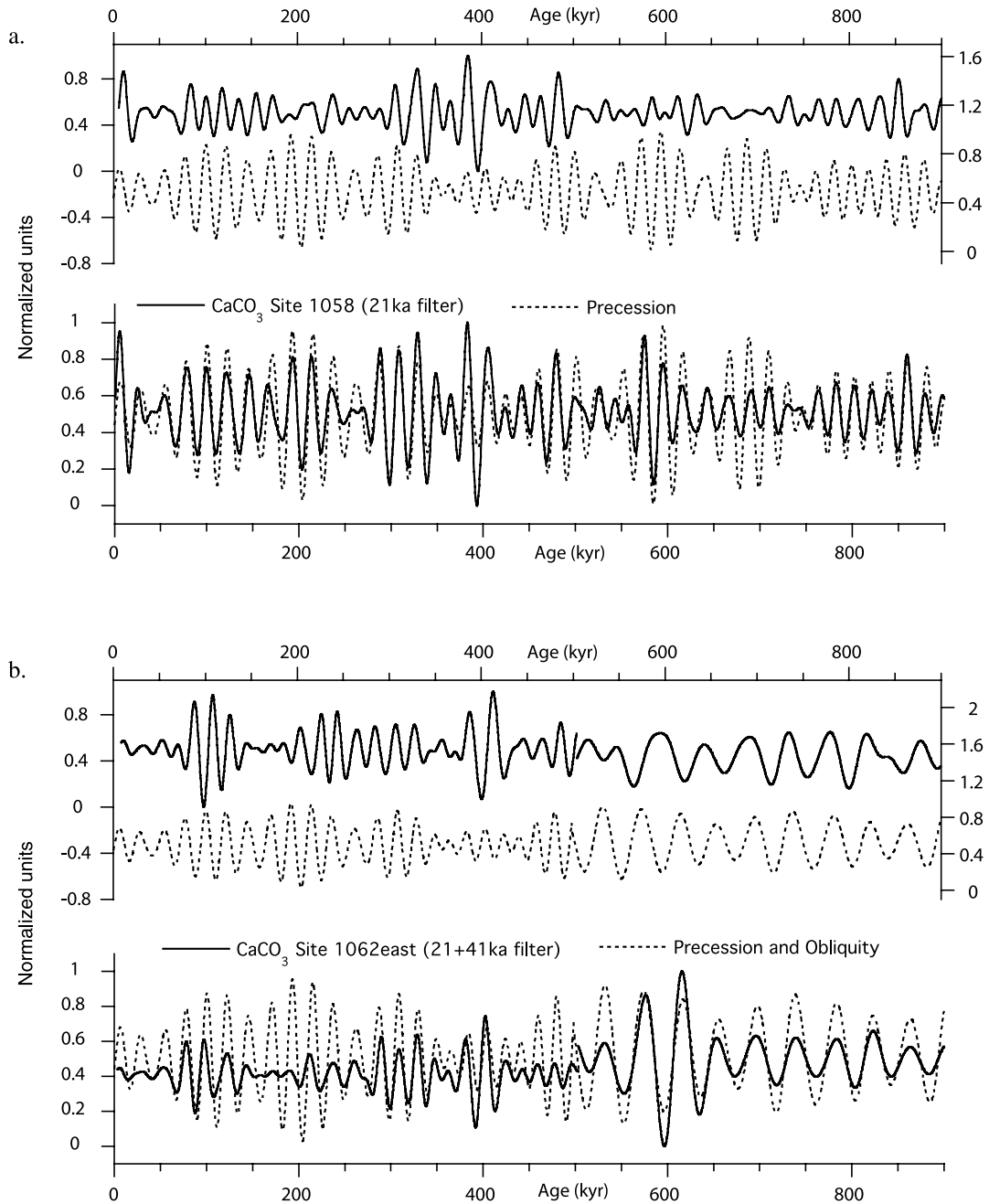


Fig. 6. Comparison of the filtered carbonate records from Sites 1058 (a) and Site 1062east (b) to the orbital target curves (precession and obliquity) before (initial age model) and after (final age model) the fine-tuning. As much as possible the tuning was done with orbital precession as a target curve because of the higher resolution. Because of very weak precession-related cycles, precession tuning was impossible for the interval 0.5–0.9 Ma at Sites 1060–1063.

resolution time scales the following strategy was used: for both of the above groups one ‘reference’ site was chosen, based on both the quality of sediment recovered and the time period covered. The reference sites are Site 1058, which was used as the reference for Sites 1055–1059, and Site 1062east, which was used as the reference for Sites 1060–1063. A short slumped interval occurred between 52.15 and 53.59 mcd (MIS 11) at Site 1058. To close this gap we used Site 1056 as a reference for MIS 11. The reference sites were dated by correlating their carbonate records (‘reference’ records) to the La90 (Laskar, 1990) orbital solutions for obliquity and precession of the Earth. Our initial target, the low latitude isotope stack (Bassinot et al., 1994) is based on an other orbital solution (Ber90; Berger and Loutre, 1991) but the differences between the solutions over the last 0.9 Ma are less than 2 kyr and could be neglected for the purpose of this study. Before the tuning we

applied phase-free digital band pass filters (centered at 21 and 41 kyr) to the reference records in order to extract precession and obliquity components from the carbonate variations. Each maximum and minimum of the filter outputs was directly correlated to its counterpart in the astronomical (obliquity or precession) records giving two age control points for each precession and obliquity cycle. All other sites (‘non-reference’ sites) in each of the two groups were dated by direct comparison with the ‘reference’ sites. First, raw carbonate data series were compared by correlating common features in ‘reference’ and ‘non-reference’ records. Afterwards, final dating was obtained by comparison of the band pass filtered carbonate records. As much as possible the tuning was done with orbital precession as a target curve, because of the higher resolution.

For Site 1058 (and all other sites of the shallow group) the 21-kyr cycles are well developed in the

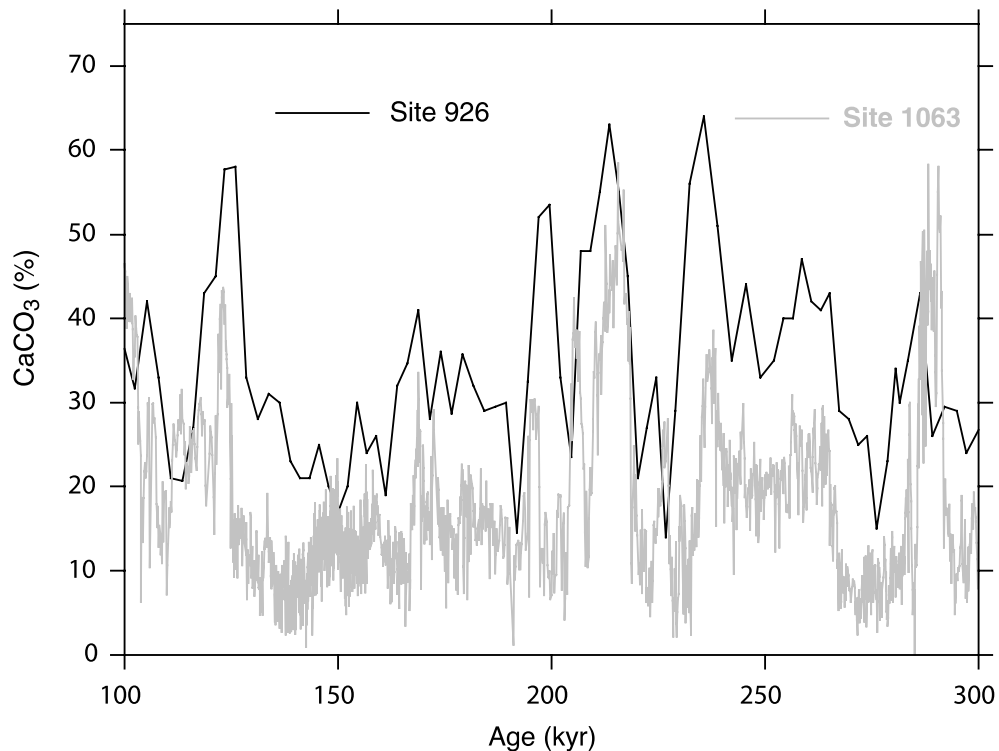


Fig. 7. Precession tuning for MIS 6–8 was difficult at the deeper Sites 1060–1063 because of weakly developed 21-kyr cycles. Therefore, tuning in this interval was supported by comparisons of the Leg 172 time series (here Site 1063, Bermuda Rise) with a carbonate record (Bickert et al., 1997) from Site 926 (Ceara Rise).

carbonate records and tuning was straightforward. Especially MIS 1–11 at these sites are characterized by a remarkable similarity between amplitude variations in orbital precession and the 21-kyr filter output from the carbonate records (Fig. 6). At Sites 1056 and 1057, deformed and convoluted beds, probably caused by multiple slumping events, were observed below 109 and 89 mcd, respectively. Because of these disturbed intervals, tuning at Sites 1056 and 1057 was only possible back to 0.82 Ma.

At the deeper sites very weak precession-related cycles were found in MIS 6 and 7. This made precession tuning very difficult in this interval because time shifts of 20 kyr resulted in very similar filter outputs and made the correlation ambiguous. Finally, a solution offering the best correlation with a lower resolution carbonate time series from ODP Site 926 at the Ceara Rise (Bickert et al., 1997) was chosen (Fig. 7). This solution is also supported by geomagnetic excursion 7A which was found close to the boundary between MIS 6 and 7 at Sites 1060–1063 (Keigwin et al., 1998). It has been shown that this excursion correlates with other marine and also continental geomagnetic records (Williams et al., submitted). According to the age model presented here, the excursion occurred at 190–195 kyr which is in good agreement with published ages for this event (e.g. Herero-Bervera et al., 1989).

The deeper sites showed low variance in the 21-kyr band for sediments older than 0.5 Ma, which made precession tuning impossible in the interval 0.5–0.9 Ma. However, 41-kyr cyclicity is well developed for this time span at all sites, which allowed easy obliquity tuning at the deeper sites, yielding an age control point about every

20 kyr. The change in spectral character at 0.5 Ma goes along with the transition from a diffuse to a more focused flow in the WBUC which could be related to the onset of strong 100-kyr cycles in the Late Pleistocene (Giosan et al., 2002). The stronger 21-kyr cyclicity at the shallower sites possibly indicates an amplification of the high latitude glacial/interglacial precessional signal by low latitude phenomena (Short et al., 1991).

Because of the direct tuning to obliquity and precession, the derived time scales are phase-locked (with zero time lag) to the target curves. However, there is a delay between orbital forcing and the response of the climate system (Imbrie and Imbrie, 1980) which was estimated to be about 5 kyr for the precessional band of $\delta^{18}\text{O}$ changes (Imbrie et al., 1984). This phase lag estimation is based on a time invariant, single-exponential ice volume model which has been applied to several orbitally tuned time scales (e.g. Imbrie et al., 1984; Bassinot et al., 1994; Martinson et al., 1987; Shackleton et al., 1990).

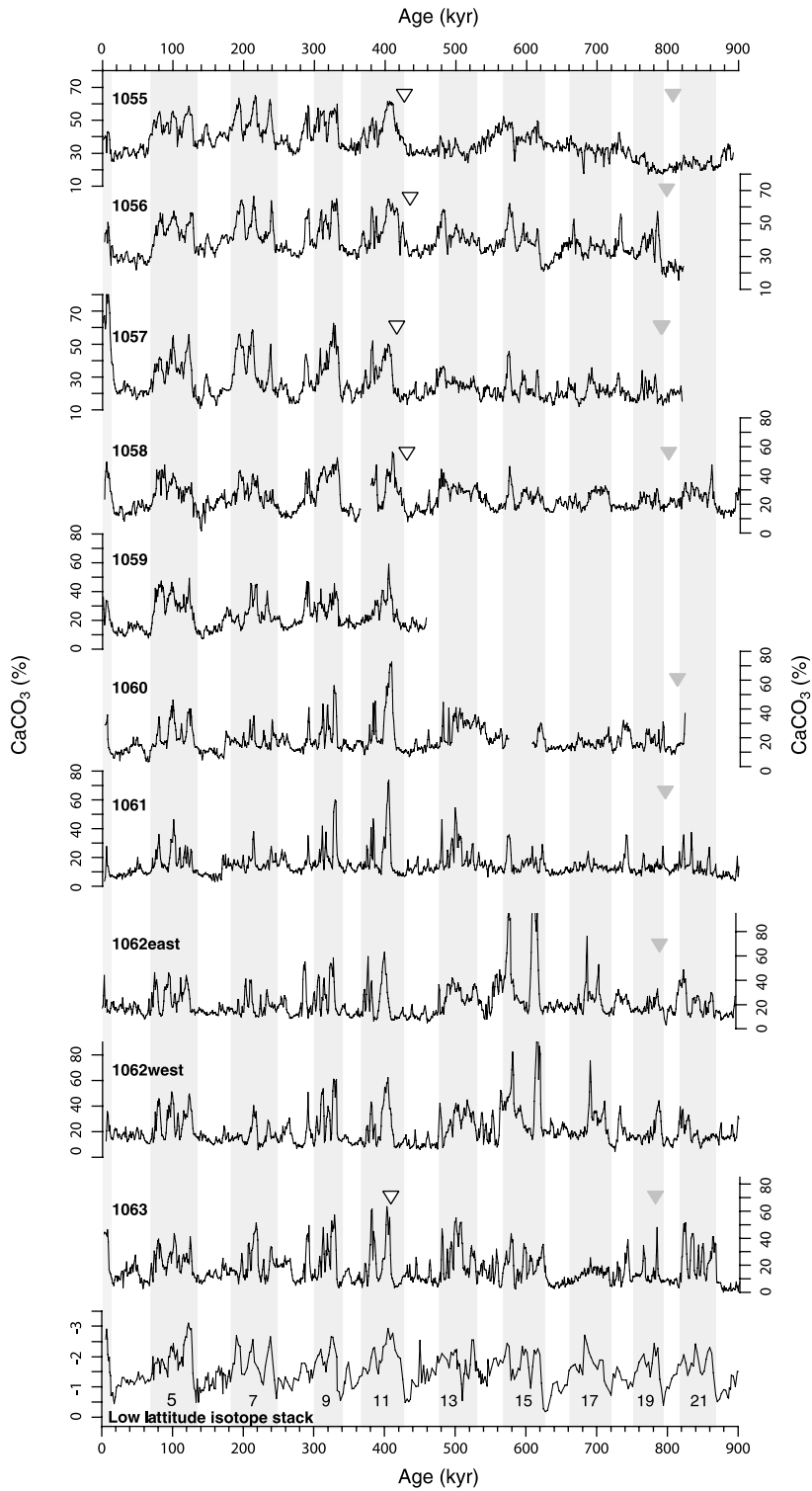
We used the available isotope data (Chaisson et al., 2002; Franz and Tiedemann, 2002) (Fig. 2) to test if there is a significant lag between carbonate and oxygen isotope curves at Site 1056. But cross spectra yielded only minor phase differences between carbonate content and oxygen isotopes (Table 1) confirming that carbonate content variations in the western North Atlantic are in phase with global ice volume changes.

According to these results, a phase lag of 5 kyr between carbonate content and insolation was adopted from Imbrie et al. (1984) and has been subtracted from the tuned ages to obtain the final age model.

Table 1
Coherencies (coh) and phase relations (in radians and kyr) of carbonate versus oxygen isotope time series (planktic and benthic) from Site 1056

Site	41 kyr			21 kyr		
	coh	(rad)	(kyr)	coh	(rad)	(kyr)
CaCO ₃ versus planktic oxygen isotopes (249–345 kyr)						
1056	0.83	−0.49	−3.3 ± 2.0	0.91	−0.47	−1.6 ± 0.7
CaCO ₃ versus benthic oxygen isotopes (341–460 kyr)						
1056	0.88	0.13	0.8 ± 1.5	0.77	0.42	1.4 ± 1.2

The 95% confidence level is at 0.80.



4. Final time series

All orbital tuned and phase-adjusted carbonate time series are shown in Fig. 8. For glacial episodes average carbonate content is consistently lower at the deeper sites, as expected from both higher dissolution and dilution with depth. Interglacial intervals display a different pattern with frequent carbonate ‘spikes’ at the deeper sites. This is especially evident for MIS 9 and 11. The high carbonate peaks (> 90%) observed for MIS 15 at Site 1062 (east and west) do not occur at the other Blake Outer Rige locations suggesting massive carbonate input from a local source during this time interval. There is a striking similarity of carbonate records from Sites 1061 (Blake Bahama Outer Ridge) and 1063 (Bermuda Rise) indicating that the pattern of sedimentation was basin-wide during the last 0.9 Ma.

The last occurrence of the nannofossil *Pseudemiliana lacunosa* was found at every drilling location and preliminary depth ranges (in mcd) for this event were derived from low resolution sampling during the cruise. At Sites 1055–1058 and 1063 refinement of the shipboard data by higher-resolution shorebased investigations (Fornaciari, Raffi, Rio, pers. commun.) is completed and according to our age models these new results yield ages between 0.407 and 0.433 Ma (Fig. 8) which is considerably younger than the age of 0.460 Ma given by Thierstein et al. (1977). A new calibration of the *P. lacunosa* datum also including data from other oceanic areas is currently in preparation (Fornaciari, Raffi, Rio, pers. commun.). At the deeper sites (Sites 1059–1062) on the Blake Bahama Outer Ridge quantitative work on the *P. lacunosa* event has not been not completed yet. Sediment reworking, poor preservation, and dilution make biohorizons more difficult to pinpoint at these locations (Shipboard Scientific Party, 1998d).

The positions of the Brunhes/Matuyama (B/M)

boundary according to shipboard magnetostratigraphy (Fig. 8) appear to be too old (around 0.8 Ma) at the shallower sites (Sites 1055–1060) compared to the latest published ages of 0.780 ± 0.01 Ma (Shackleton et al., 1990; Baksi et al., 1992) for this event. At these locations the boundary plots in an interval of low carbonate content clearly indicating a glacial period. However, based on revised isotope chronologies (Shackleton et al., 1990; deMenocal et al., 1990; Bassinot et al., 1994) the B/M transition occurred during interglacial MIS 19. Polarity assessment during Leg 172 was difficult at sites in shallow and intermediate water depth due to overprint, reduction diagenesis and disturbance caused by gas expansion (Keigwin et al., 1998). A further uncertainty in the stratigraphic position of the B/M reversal can result from post-depositional remanent magnetization (Kent, 1973), with the Earth’s magnetic field affecting sediments a few cm below the sediment-water interface. Estimates of this ‘lock-in depth’ vary from 7 to 16 cm (e.g. deMenocal et al., 1990; Schneider et al., 1992). Based on these numbers and the high sedimentation rates at the drift locations we estimate the resulting shift of the B/M boundary caused by the ‘lock-in effect’ to be in the order of only a few kyr. Thus we conclude that the age discrepancy for the B/M boundary is not caused by the age models but rather by uncertainties in the shipboard polarity stratigraphy. This is also supported by magnetostratigraphy at Site 1063 on the Bermuda Rise where polarity reversals were most easily identified (M. Okada, pers. commun.) and the B/M boundary plots exactly between 0.780 Ma (Hole 1063A) and 0.782 Ma (Holes 1063B and 1063C).

Cross spectral analyses (Fig. 9) show that variance in the tuned time series of carbonate content is distributed over all the main orbital frequencies. At these frequencies the carbonate records are highly (> 95%) coherent with the low latitude isotope stack of Bassinot et al. (1994).

Fig. 8. Carbonate content records of Sites 1055–1063 versus tuned and phase-adjusted age. Open triangles mark the last occurrence of nannofossil *P. Lacunosa* according to the depth range determined by a quantitative postcruise study (Fornaciari, Raffi, Rio, pers. commun.). The B/M magnetic reversal (closed triangles) is plotted with respect to its position determined during the cruise.

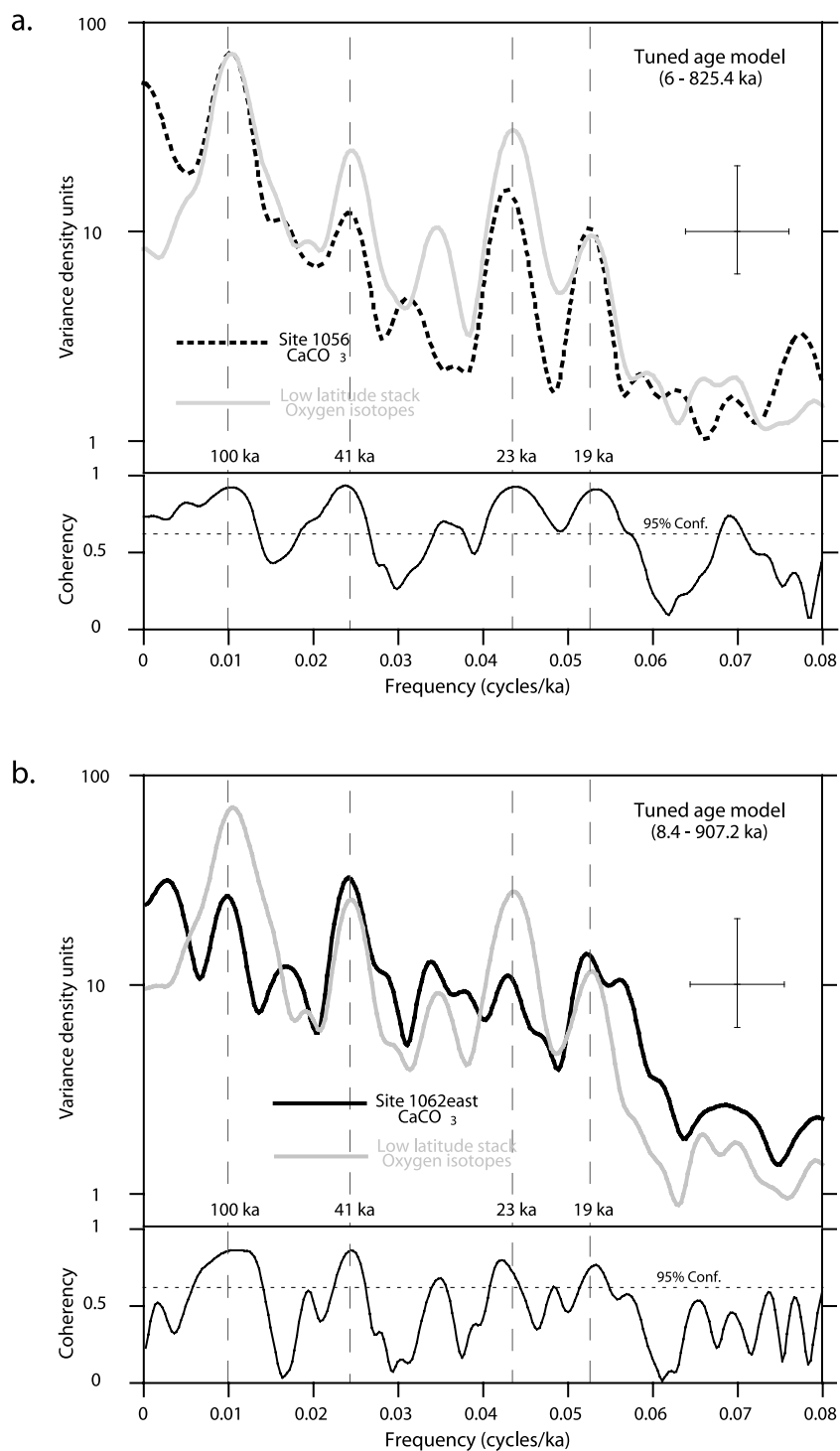


Fig. 9. Cross spectral analyses of the tuned carbonate time series from Sites 1056 (a) and 1062east (b) relative to the low latitude isotope stack of Bassinot et al. (1994). The Blackman–Tuckey approach with 30% lags was used.

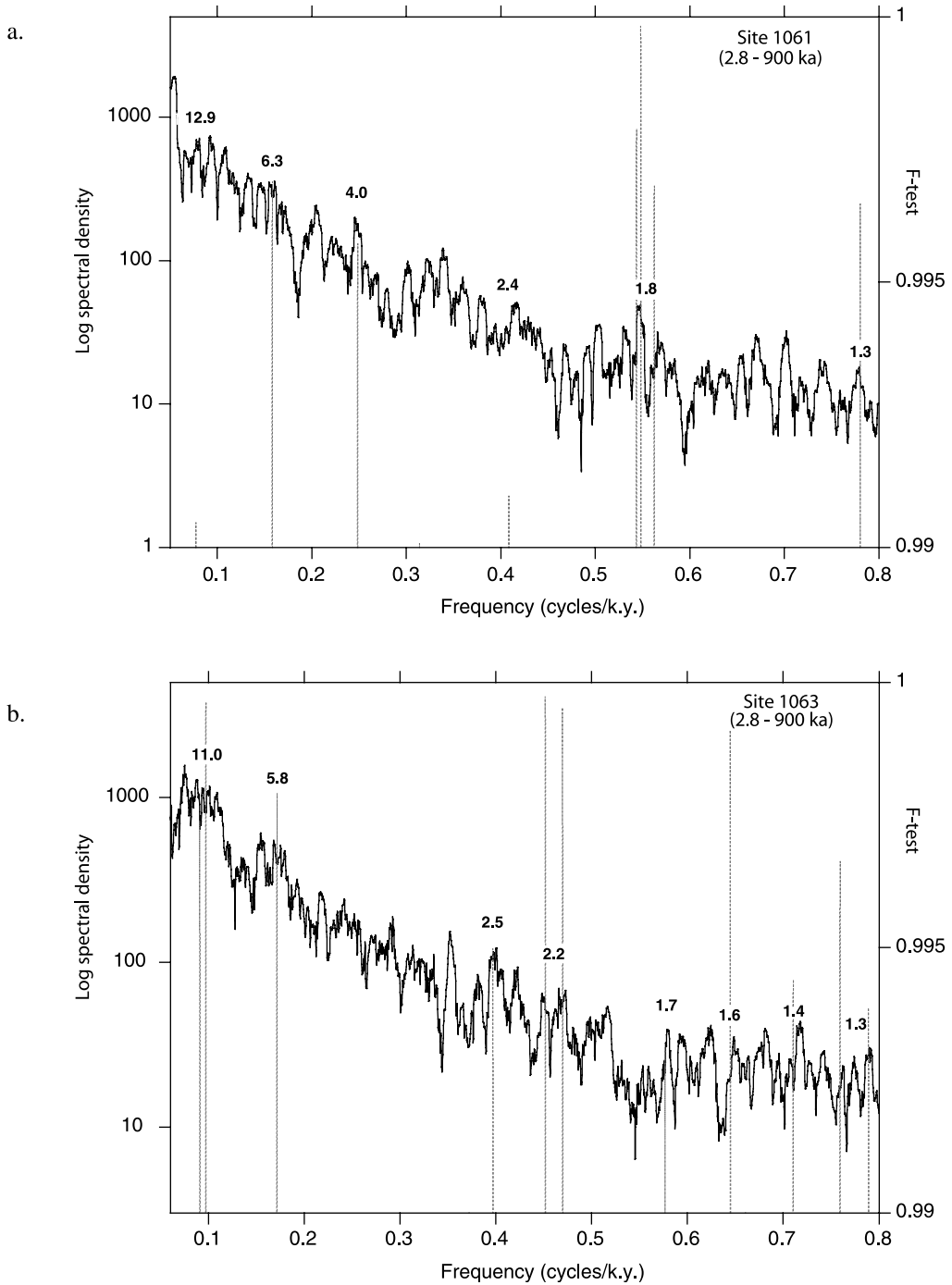


Fig. 10. MTM spectral analyses of carbonate time series from Sites 1061 (Blake Bahama Outer Ridge) and 1063 (Bermuda Rise). The sub-Milankovitch frequency band is shown. Only periods with a significance of >0.99 (dashed lines) are used for interpretation.

Table 2
Final age models for Sites 1055–1059

Tuned age (ka)	Phase-adjusted age (ka)	1055 depth	1056 depth	1057 depth	1058 depth	1059 depth
0.0	0.0	0.00	0.00	0.00	0.00	0.00
6.0	1.0	0.22	0.09	0.14	0.09	0.06
9.6	4.6	0.97	0.30	0.16	0.27	0.09
22.8	17.8	5.26	3.42	0.92	2.32	3.30
35.2	30.2	8.41	5.78	1.97	5.11	8.49
56.8	51.8	11.55	8.13	5.83	11.61	20.74
71.2	66.2	13.09	9.48	10.50	17.32	24.90
82.4	77.4	14.86	10.61	11.65	18.99	28.15
94.0	89.0	16.81	11.61	12.09	20.16	30.48
104.4	99.4	18.90	12.38	12.53	21.07	33.40
114.8	109.8	20.10	12.96	12.99	22.16	35.50
127.2	122.2	23.14	13.83	13.56	23.40	37.67
140.4	135.4	26.64	15.48	15.33	26.57	40.59
149.6	144.6	29.48	17.76	17.58	27.86	44.35
162.0	157.0	31.80	19.80	19.16	29.03	48.63
175.2	170.2	32.86	20.16	19.84	30.14	51.85
186.8	181.8	33.71	20.53	19.96	32.23	53.97
197.2	192.2	34.47	20.97	20.31	33.00	56.23
207.6	202.6	35.51	21.52	20.53	33.29	58.06
218.8	213.8	37.23	22.33	20.82	33.58	61.31
230.4	225.4	39.13	22.85	21.40	34.25	62.90
242.8	237.8	42.09	23.63	21.99	35.03	65.03
263.6	258.6	45.56	26.27	23.77	39.21	69.46
278.8	273.8	47.79	27.95	25.76	41.27	72.42
292.0	287.0	50.42	29.63	27.63	43.00	74.85
312.8	307.8	55.39	31.46	29.17	44.61	77.66
333.6	328.6	59.75	33.75	30.49	46.22	79.85
344.8	339.8	62.24	35.72	31.12	47.18	81.48
353.6	348.6	64.78	37.29	32.58	48.36	82.77
359.2	354.2	65.88	38.29	33.35	49.44	83.82
370.4	365.4	68.11	40.31	36.24	50.77	86.78
380.0	375.0	69.46	40.95	37.19	51.82	89.06
387.6	382.6	70.47	41.45	37.70	53.07	90.52
397.2	392.2	72.76	42.18	38.22	54.38	91.75
409.6	404.6	75.78	43.03	39.04	56.08	94.50
427.6	422.6	78.65	44.16	40.66	58.35	97.19
436.8	431.8	79.33	44.79	41.56	59.36	97.85
447.2	442.2	80.33	46.59	42.23	60.81	98.58
463.6	458.6	82.37	49.06	44.06	62.76	100.59
474.0	469.0	83.45	51.75	45.39	63.94	
484.4	479.4	84.24	53.31	46.77	65.52	
494.8	489.8	85.15	54.65	47.84	67.04	
506.0	501.0	85.83	55.95	48.42	68.68	
514.4	509.4	86.05	56.76	48.76	71.27	
530.8	525.8	86.69	58.90	50.26	72.78	
547.6	542.6	87.67	61.20	52.56	74.64	
556.4	551.4	89.15	62.25	53.32	77.42	
565.6	560.6	90.51	63.36	54.12	78.72	
578.0	573.0	91.95	64.96	55.33	80.14	
589.6	584.6	93.23	65.92	55.86	80.82	
598.8	593.8	94.17	66.54	56.29	81.42	
610.4	605.4	95.64	67.73	57.42	82.75	
620.8	615.8	97.17	69.25	58.48	83.85	

Table 2 (Continued).

Tuned age (ka)	Phase-adjusted age (ka)	1055 depth	1056 depth	1057 depth	1058 depth	1059 depth
632.0	627.0	98.08	71.09	59.87	85.06	
650.0	645.0	99.66	74.09	61.19	85.61	
659.6	654.6	100.47	76.30	61.57	86.07	
670.0	665.0	101.26	80.82	62.04	86.62	
682.4	677.4	102.35	84.28	63.54	87.23	
692.8	687.8	103.18	85.82	66.13	89.45	
703.2	698.2	104.17	87.29	68.72	92.32	
713.6	708.6	105.14	89.15	71.16	93.64	
723.2	718.2	106.22	91.67	73.30	94.84	
735.2	730.2	106.96	94.68	75.62	95.42	
749.6	744.6	108.22	96.88	78.35	96.09	
760.0	755.0	109.67	98.59	79.73	96.48	
767.6	762.6	110.60	99.46	80.80	97.47	
777.2	772.2	111.45	100.99	82.14	99.86	
787.6	782.6	112.41	103.40	84.08	102.00	
798.0	793.0	113.19	104.66	85.59	103.27	
806.4	801.4	114.02	105.98	86.90	104.17	
816.0	811.0	114.82	107.63	88.12	105.18	
825.6	820.6	115.99	108.70	88.84	105.97	
836.0	831.0	116.73			106.53	
844.4	839.4	117.14			106.96	
854.0	849.0	117.74			107.39	
864.4	859.4	118.42			107.96	
875.6	870.6	119.17			108.89	
885.2	880.2	120.00			110.92	
899.6	894.6	121.46			114.75	

Depth is given in meters composite depth (Keigwin et al., 1998).

5. An application: the detection of sub-Milankovitch climatic variability

The deep water Sites 1061 (4050 m water depth) and 1063 (4570 m water depth) were chosen to study millennial-scale climatic variability in the western North Atlantic. Both sites show very high and variable sedimentation rates (23.4 ± 13.0 cm/kyr at Site 1061 and 19.2 ± 12.0 at Site 1063) over the last 0.9 Ma and allow comparison of the sub-Milankovitch spectral pattern from the Blake Outer Ridge (Site 1061) to that from the Bermuda Rise (Site 1063). The sample interval of 2–4 cm for the carbonate predictions resulted in average time resolutions of 171 yr (110–385 yr) at Site 1061 and 208 yr (128–556 yr) at Site 1063. Thus the lowest theoretical period that can be resolved (Nyquist period) is always below 1112 yr (two times maximum sampling period). However, sedimentological records in general are

not ideal time series and could be disturbed by bioturbation, diagenesis, etc. Therefore, periodicities lower than 3–4 times the sampling period (1500–2000 yr in this case) should be considered with caution.

To detect millennial-scale climatic variability in the Leg 172 carbonate records we performed multi taper method (MTM) spectral analyses (Thompson, 1982). The purpose of the MTM is to compute a set of independent and significant estimates of the power spectrum, in order to obtain a better and more reliable estimate than with traditional (e.g. Blackman–Tuckey) techniques. Spectra were calculated by using seven tapers and a time bandwidth resolution of four. This setting was used to provide good resolution at sub-Milankovitch (< 19 kyr) periodicity. The calculations were done with the Analyseries software by Paillard et al. (1996). The MTM harmonic analyses estimates also provide a statistical

Table 3
Final age models for Sites 1060–1063

Tuned age (ka)	Phase-adjusted age (ka)	1060 depth	1061 depth	1062east depth	1062west depth	1063 depth
0.0	0.0	0.00	0.00	0.00	0.00	0.00
6.0	1.0	0.05	0.07	0.04	0.05	0.07
9.6	4.6	0.09	0.09	0.07	0.08	0.10
22.8	17.8	6.84	4.07	3.07	2.70	7.45
35.2	30.2	13.00	9.46	6.39	5.81	16.18
56.8	51.8	20.44	19.18	10.53	9.84	24.18
71.2	66.2	30.29	27.02	14.77	13.10	27.81
82.4	77.4	34.35	30.93	17.39	15.25	30.26
94.0	89.0	37.04	32.96	19.32	16.94	31.28
104.4	99.4	38.37	34.44	20.57	18.10	33.25
114.8	109.8	39.27	35.74	21.85	19.24	34.65
127.2	122.2	40.75	37.49	22.67	20.25	35.96
140.4	135.4	42.09	41.21	23.89	21.96	38.62
149.6	144.6	44.41	44.37	24.73	23.25	41.67
162.0	157.0	52.54	49.67	28.58	25.94	47.59
175.2	170.2	61.02	55.69	31.48	29.29	50.76
186.8	181.8	65.13	59.95	33.95	31.40	52.92
197.2	192.2	68.16	62.29	35.73	32.22	54.04
207.6	202.6	70.21	64.63	37.50	33.04	55.16
218.8	213.8	72.32	67.04	39.31	33.73	56.58
230.4	225.4	75.62	69.38	41.24	34.39	58.12
242.8	237.8	78.40	71.44	43.82	35.47	60.03
263.6	258.6	81.54	74.91	46.74	37.53	63.14
278.8	273.8	87.06	80.29	49.30	39.00	65.79
292.0	287.0	91.86	85.87	51.75	40.15	68.87
312.8	307.8	97.18	91.07	54.43	41.93	71.75
333.6	328.6	100.61	95.18	57.55	43.97	74.83
344.8	339.8	103.97	96.66	58.49	45.13	77.45
353.6	348.6	106.87	99.00	60.03	46.07	80.46
359.2	354.2	108.43	101.69	60.58	46.64	82.22
370.4	365.4	111.01	107.44	62.24	47.78	84.84
380.0	375.0	115.08	110.13	63.50	48.86	87.01
387.6	382.6	118.59	112.73	64.54	49.71	88.06
397.2	392.2	119.26	113.67	65.11	50.34	88.55
409.6	404.6	120.08	114.72	66.29	50.93	90.44
427.6	422.6	123.36	118.46	68.58	52.95	96.47
436.8	431.8	125.56	121.49	69.91	54.11	100.11
447.2	442.2	127.39	125.40	71.17	55.21	102.25
463.6	458.6	135.77	127.66	72.15	56.13	103.92
474.0	469.0	137.52	129.15	72.85	56.53	104.73
484.4	479.4	139.33	131.61	73.50	56.86	105.74
494.8	489.8	141.00	133.08	74.94	57.70	106.85
506.0	501.0	142.14	134.46	76.94	58.43	108.52
516.9	511.9	143.60	136.87	78.26	60.04	111.98
536.8	531.8	144.77	139.09	79.28	62.35	113.90
557.3	552.3	146.13	140.88	81.04	64.89	115.37
578.8	573.8	148.81	142.33	83.18	65.80	116.63
601.4	596.4	151.73	143.93	83.79	66.32	118.40
621.7	616.7	154.41	146.05	84.36	66.84	120.20
641.1	636.1	155.73	148.33	85.06	67.52	121.80
660.6	655.6	156.71	150.42	86.79	68.44	124.27
680.9	675.9	159.14	152.38	89.14	67.40	127.47
702.8	697.8	161.77	154.74	91.30	70.66	131.81

Table 3 (Continued).

Tuned age (ka)	Phase-adjusted age (ka)	1060 depth	1061 depth	1062east depth	1062west depth	1063 depth
722.9	717.9	164.18	157.78	93.77	72.41	135.48
743.7	738.7	166.97	161.07	95.03	73.87	138.05
766.3	761.3	170.01	164.49	96.32	74.98	142.29
788.9	783.9	174.40	170.42	99.27	76.20	150.96
808.8	803.8	178.94	177.06	101.96	77.58	155.45
827.5	822.5	182.50	180.23	102.95	79.23	158.05
848.1	843.1		182.73	103.83	80.76	160.08
868.4	863.4		184.60	104.77	81.96	161.93
889.4	884.4		188.68	106.96	83.22	164.22
910.4	905.4		199.54	108.93	84.36	167.02

Depth is given in meters composite depth (Keigwin et al., 1998).

significance test (Fisher or F test) for the amplitude spectrum (e.g. Yiou et al., 1997).

The MTM spectra from Sites 1061 and 1063 for the sub-Milankovitch frequency band show a variety of spectral density maxima (Fig. 10) but for the interpretation we shall consider only peaks with very high significance (F test > 0.99). At both sites the significant periods group around 11–12, 6, 2.2–2.5, and 1.3–1.8 kyr, again indicating a basin-wide similar sedimentary regime. Furthermore, significant variance at 4.0 kyr characterizes the record from Site 1061. At the Bermuda Rise the significance of the 4-kyr period is also high (0.94) although it does not exceed the 0.99 level. The variations of periods around the detected peaks, especially at shorter periods, are most likely due to uncertainties in the age models caused by variable sedimentation rates between age control points. Previous studies of marine sediments and ice cores (e.g. Hagelberg et al., 1994; Yiou et al., 1995; Cortijo et al., 1995; Ortiz et al., 1999) found periodicities similar to the ones described here.

In all investigations a strong cyclicity at 10–12 kyr was found, which could arise as a second-order precessional harmonic (e.g. Hagelberg et al., 1994). Cyclicities of 5–8 kyr have been attributed to quasi-periodic Heinrich events by Cortijo et al. (1995) who performed MTM analyses on two gray scale time series (Cores SU90-08 and SU90-39) from the central North Atlantic covering the last 0.3 Ma. The deuterium isotope record from Vostok (Antarctica) displays a 6-kyr cyclicity (Yiou et al., 1997) which is close to the behav-

ior predicted by ice sheet oscillation models (e.g. MacAyeal, 1993). Ortiz et al. (1999) found spectral peaks around 6 and 8 kyr throughout the last 4.5 Ma in a record of estimated carbonate content from the Feni Drift. They demonstrated that a rectified precession record could translate variance from the 19–23-kyr doublets to both longer and shorter frequency responses with sub-Milankovitch variability at 9.6–11.6, 6.7–8.6 and 5.2–5.8 kyr. An example for a physical explanation of this phenomenon was given by Short et al. (1991) who postulated that low latitude equatorial regions are influenced twice for each precessional maximum (minimum) because the responses of the Northern and Southern Hemispheres to orbital variations are out of phase. Thus the occurrence of significant peaks in the carbonate records from Sites 1061 and 1063 in frequency bands which are similar to that observed in the clipped precession record (Ortiz et al., 1999) indicates that at least some of the variance in the carbonate sedimentation in the western Atlantic may be non-linearly forced by precession.

The high-resolution records obtained during Leg 172 allow also to detect higher frequency cyclicities with periods below 5 kyr: 2.5–4-kyr cycles as seen in the records from Sites 1061 and 1063 have been detected in Greenland ice cores (Dansgaard–Oeschger cycles) and were also recognized by Keigwin and Jones (1994) who analyzed giant piston cores from western Atlantic drifts. Although the spectral peaks at 1.3–1.8 kyr are close to the Nyquist period (see above) for some short intervals with lower sedimentation rate, they

clearly indicate millennial-scale variations in carbonate deposition on the Blake Bahama Outer Ridge and the Bermuda Rise. Such climatic cycles of about 1.5-kyr duration were also found in North Atlantic sediments of Holocene (Bond et al., 1997), Late Pleistocene (Oppo et al., 1998), and Early Pleistocene age (Raymo et al., 1998). The fact that these periods, as most of the higher frequency cycles, appear in different areas and at various time intervals suggests that sub-Milankovitch climatic variability was relatively pervasive during the Pleistocene and only weakly coupled to the intensification of Northern Hemisphere glaciation (Ortiz et al., 1999). With advanced evolutionary spectral methods it should be possible to gain further insights into the developments of these cyclicities over time.

Possible other applications of the age models are manifold. Together with high-resolution geochemical and sedimentological analyses the derived time scales (Tables 2 and 3) can provide the basis for detailed paleoceanographic studies in the westernmost Atlantic. They will also allow detailed inter-site comparisons based on accumulation rates of biogenous and terrigenous sediment components as well as regional and global correlations to other drill sites.

Acknowledgements

We acknowledge the work done by the crew of the JOIDES Resolution for the acquisition of the cores. This research used samples and data provided by the Ocean Drilling Program (ODP). The ODP is sponsored by the U.S. National Science Foundation (NSF) and participating countries under management of Joint Oceanographic Institutions (JOI), Inc. We thank F.J. Hilgen and one anonymous reviewer for their constructive criticism that significantly improved the paper.

References

- Baksi, A.K., Hsu, V., McWilliams, M.O., Farrar, E., 1992. $^{40}\text{Ar}/^{39}\text{Ar}$ dating of the Brunhes–Matuyama geomagnetic field reversal. *Science* 256, 356–357.
- Bassinot, F.C., Labeyrie, L.D., Vincent, E., Quidelleur, X., Shackleton, N.J., Lancelot, Y., 1994. The astronomical theory of climate and the age of the Brunhes–Matuyama magnetic reversal. *Earth Planet. Sci. Lett.* 126, 91–108.
- Berger, A., Loutre, M.F., 1991. Insolation values for the climate of the last 10 million years. *Quat. Sci. Rev.* 10, 297–317.
- Berger, W.H., Bickert, T., Wefer, G., Yasuda, M.K., 1995. Brunhes–Matuyama boundary: 790 k.y. date consistent with ODP Leg 130 oxygen isotope records based on fit to Milankovitch template. *Geophys. Res. Lett.* 22, 1525–1528.
- Bickert, T., Curry, W.B., Wefer, G., 1997. Late Pliocene to Holocene (2.6–0 Ma) Western Equatorial Atlantic deep-water circulation: inferences from benthic stable isotopes. In: Shackleton, N.J., Curry, W.B., Richter, C., Bralower, T.J. (Eds.), *Proc. ODP Sci. Results 154*. ODP, College Station, TX, pp. 239–254.
- Bond, G., Showers, W., Cheseby, M., Lotti, R., Almasi, P., deMenocal, P., Priori, P., Cullen, H., Hajdes, I., Bonani, G., 1997. A pervasive millennial-scale cycle in North Atlantic Holocene and Glacial climates. *Science* 278, 1257–1266.
- Chaisson, W.P., Poli, M.-S., Thunell, R.C., 2002. Gulf stream and Western Boundary undercurrent variations during MIS 10/12 at site 1056, Blake Bahama Outer Ridge. *Mar. Geol.* 189, S0025-3227(02)00324-9.
- Cortijo, E., Yiou, P., Labeyrie, L., Cremer, M., 1995. Sedimentary record of rapid climate variability in the North Atlantic Ocean during the last glacial cycle. *Paleoceanography* 10, 911–926.
- deMenocal, P.B., Ruddiman, W.F., Kent, D.V., 1990. Depth of post-depositional remanence acquisition in deep-sea sediments: a case study of the Brunhes–Matuyama reversal and oxygen isotopic Stage 19.1. *Earth Planet. Sci. Lett.* 99, 1–13.
- Franz, S.O., Tiedemann, R., 2002. Depositional changes along the Blake–Bahama Outer Ridge deep water transect during marine isotope stage 8 to 10 – links to the Deep Western Boundary Current (DWBC). *Mar. Geol.* 189, S0025-3227(02)00325-0.
- Giosan, L., Flood, R.D., Grützner, J., Franz, S.-O., Poli, M.-S., Hagen, S., 2001. High-resolution carbonate content estimated from diffuse spectral reflectance for Leg 172 sites. In: Keigwin, L.D., Rio, D., Acton, G.D., Arnold, E. (Eds.), *Proc. ODP Sci. Results 172* (On-line). Available from World Wide Web: http://www-odp.tamu.edu/publications/172_SR/chap_06/chap_06.htm.
- Giosan, L., Flood, R.D., Aller, R., 2002. Paleoclimatological significance of sediment color on western North Atlantic drifts: I. Origin of color. *Mar. Geol.* 189, S0025-3227(02)00321-3.
- Hagelberg, T.K., Bond, G., deMenocal, P., 1994. Milankovitch band forcing of sub-Milankovitch climate variability during the Pleistocene. *Paleoceanography* 9, 545–558.
- Hays, J.D., Imbrie, J., Shackleton, N.J., 1976. Variations in the earth's orbit: Pacemaker of the ice ages. *Science* 194, 1121–1132.
- Herrero-Bervera, E.C.E., Helsley, S.R., Hammond, L.A., Chitwood, A., 1989. Possible lacustrine paleomagnetic record of

- the Blake episode from Pringle Falls, Oregon, USA. *Phys. Earth Planet. Int.* 56, 112–123.
- Imbrie, J., Imbrie, J.Z., 1980. Modeling the climatic response to orbital variations. *Science* 207, 943–953.
- Imbrie, J., Hays, J.D., Martinson, D.G., McIntyre, A., Mix, A.C., Morley, J.J., Pisias, N.G., Prell, W.L., Shackleton, N.J., 1984. The orbital theory of Pleistocene climate: support from a revised chronology of the marine $\delta^{18}\text{O}$ record. In: Berger, A., Imbrie, J., Hays, J., Kukla, G., Saltzman, B. (Eds.), *Milankovitch and Climate* (Pt. 1). Plenum Reidel, Dordrecht, pp. 269–305.
- Johnson, R.G., 1982. Brunhes–Matuyama magnetic reversal dated at 790 000 yr B.P. by marine-astronomical correlations. *Quat. Res.* 17, 135–147.
- Keigwin, L.D., Jones, G.A., 1994. Western North Atlantic evidence for millennial-scale changes in ocean circulation and climate. *J. Geophys. Res.* 99, 12397–12410.
- Keigwin, L.D., Rio, D., Acton, G. et al., 1998. Proc. ODP Init. Rep. 172. ODP, College Station, TX.
- Kent, D.V., 1973. Post-depositional remanent magnetization in deep-sea sediment. *Nature* 246, 32–33.
- Laskar, J., 1990. The chaotic motion of the solar system: a numerical estimation of the size of the chaotic zones. *Icarus* 88, 266–291.
- MacAyeal, D.R., 1993. A low-order model of the Heinrich event cycle. *Paleoceanography* 8, 767–773.
- Martinson, D.G., Pisias, N., Hays, J.D., Imbrie, J., Moore, T.C., Shackleton, N.J., 1987. Age dating and the orbital theory of the ice ages: development of a high-resolution 0 to 300 000-year chronostratigraphy. *Quat. Res.* 27, 1–30.
- Milankovitch, M., 1920. *Théorie Mathématique des Phénomènes Thermiques Produits par la Radiation Solaire*. Gauthiers-Villars, Paris.
- Milankovitch, M., 1941. Kanon der Erdbestrahlung und das Eiszeitenproblem. *R. Serb. Acad. Spec. Publ.* 133, 1–633.
- Oppo, D.W., McManus, J.F., Cullen, J.L., 1998. Abrupt climate events 500 000 to 340 000 years ago: evidence from subpolar North Atlantic sediments. *Science* 279, 1335–1338.
- Ortiz, J., Mix, A., Harris, S., O'Connell, S., 1999. Diffuse spectral reflectance as a proxy for percent carbonate content in North Atlantic sediments. *Paleoceanography* 14, 171–186.
- Paillard, D., Labeyrie, L., Yiou, P., 1996. Macintosh program performs time-series analysis. *Eos Trans. Am. Geophys. Union* 77, 379.
- Raymo, M.E., Ganley, K., Carter, S., Oppo, D.W., McManus, J., 1998. Millennial-scale climate instability during the early Pleistocene epoch. *Nature* 392, 699–702.
- Schneider, D.A., Kent, D.V., Mello, G.A., 1992. A detailed chronology of the Australian impact event, the Brunhes–Matuyama geomagnetic polarity reversal, and global climate change. *Earth Planet. Sci. Lett.* 111, 395–405.
- Schwartz, M., Lund, P.S., Hammond, D.E., 1997. Early sediment diagenesis on the Blake/Bahama Outer Ridge, North Atlantic Ocean, and its effects on sediment magnetism. *J. Geophys. Res.* 102, 7903–7914.
- Shackleton, N.J., Berger, A., Peltier, W.R., 1990. An alternative astronomical calibration of the lower Pleistocene time-scale based on ODP Site 677. *Trans. R. Soc. Edinburgh Earth Sci.* 81, 251–261.
- Shackleton, N.J., Crowhurst, S.J., Hagelberg, T., Pisias, N.G., Schneider, D.A., 1995. A new late Neogene time scale: application to Leg 138 sites. In: Pisias, N.G., Mayer, L.A., Janecek, T.R., Palmer-Julson, A., van Andel, T.H. (Eds.), *Proc. ODP Sci. Results 138*. ODP, College Station, TX, pp. 73–101.
- Shipboard Scientific Party, 1998a. Explanatory notes. In: Keigwin, L.D., Rio, D., Acton, G.D. et al. (Eds.), *Proc. ODP Init. Rep. 172*. ODP, College Station, TX, pp. 13–29.
- Shipboard Scientific Party, 1998b. Summary. In: Keigwin, L.D., Rio, D., Acton, G.D. et al. (Eds.), *Proc. ODP Init. Rep. 172*. ODP, College Station, TX, pp. 311–321.
- Shipboard Scientific Party, 1998c. Intermediate depth Blake Outer Ridge, Sites 1056, 1057, 1058, and 1059. In: Keigwin, L.D., Rio, D., Acton, G.D. et al. (Eds.), *Proc. ODP Init. Rep. 172*. ODP, College Station, TX, pp. 77–156.
- Shipboard Scientific Party, 1998d. Deep Blake-Bahama Outer Ridge, Sites 1060, 1061, and 1062. In: Keigwin, L.D., Rio, D., Acton, G.D. et al. (Eds.), *Proc. ODP Init. Rep. 172*. ODP, College Station, TX, pp. 157–250.
- Short, D.A., Mengel, J.G., Crowley, T.J., Hyde, W.T., North, G.R., 1991. Filtering of Milankovitch cycles by Earth's geography. *Quat. Res.* 35, 157–173.
- Thierstein, H.R., Geitzenauer, K., Molfino, B., Shackleton, N.J., 1977. Global synchronicity of late Quaternary coccolith datum levels: validation by oxygen isotopes. *Geology* 5, 400–404.
- Thompson, D.J., 1982. Spectrum estimation and harmonic analysis. *Proc. IEEE* 70, 1055–1096.
- Tiedemann, R., Franz, S.O., 1997. Deep-water circulation, chemistry, and terrigenous sediment supply in the equatorial Atlantic during the Pliocene, 3.3–2.6 Ma and 5–4.5 Ma. In: Shackleton, N.J., Curry, W.B., Richter, C., Bralower, T.J. (Eds.), *Proc. ODP Sci. Results 154*. ODP, College Station, TX, pp. 299–318.
- Tiedemann, R., Sarntheim, M., Shackleton, N.J., 1994. Astronomic timescale for the Pliocene Atlantic $\delta^{18}\text{O}$ and dust flux records of Ocean Drilling Program site 659. *Paleoceanography* 9, 619–638.
- Williams, T., Lund, S., Acton, G., Clement, B., Okada, M., Hastedt, M., submitted. Sedimentary records of 3 geomagnetic excursions during $\delta^{18}\text{O}$ Stages 7 and 8, from the Blake Ridge, North Atlantic, ODP Leg 172. *Earth Planet. Sci. Lett.*
- Yiou, P., Jouzel, J., Johnsen, S., Røgnvaldsson, Ö.E., 1995. Rapid oscillations in Vostok and GRIP ice cores. *Geophys. Res. Lett.* 22, 2179–2182.
- Yiou, P., Fuhrer, K., Meeker, L.D., Jouzel, J., Johnson, S., Mayewski, P.A., 1997. Paleoclimatic variability inferred from the spectral analysis of Greenland Antarctic ice-core data. *J. Geophys. Res.* 102, 26441–26454.